Incorporating Optimization to Improve Durability of A356 Metal Matrix Composites with Nanoparticles of TiO2 and SiC

P. Dinesh[1], P D Jeyakumar[2*], R G Geethu Mani[3]

[1]B S A Crescent Institute of science and technology, E-Mail: dineshpaulraj@gmail.com
[2]B S A Crescent Institute of science and technology, E-Mail: pdjeyakumar@gmail.com
[3]K C G College of Technology, E-Mail: geethu jeyakumar@gmail.com

This research evaluates adaptive and statistical techniques to enhance the wear behaviour of A356 metal matrix composites supplemented by nanoparticles of TiO2 and SiC. The composites were created by the stir casting technique, and their wear behaviour was studied using a pin-on-disc device. Scanning electron microscopy (SEM) analysis confirmed an even distribution of strengthening particles over the A356 aluminum matrix surface. This research revealed that the addition of these SiC and TiO2 nanoparticles to composites resulted in a more refined particulate structure in the end product. For an examination of the composites' wear behaviour in contrast to basic alloy, the data was optimized using the Taguchi approach and Improved particle swarm optimization (I.P.S.O.) algorithm. The findings indicated that speed, applied load and sliding distance significantly influenced the rate of wear for the base alloy matrix, A356 containing 3% TiO2 nanocomposite, and A356 containing 3% SiC nanocomposite, correspondingly. Composites using nanoparticles of SiC and TiO2 have much improved tribological characteristics.

Keywords: TiO2, Nanoparticles, SEM, EBSD, IPSO.

1. Introduction

One kind of composite material is the aluminium metal matrix composite (AMMC), which is composed of an aluminium matrix reinforced with different types of particles or fibers. The excellent strength-to-weight ratio of these composites makes them useful in an extensive range of aeronautical, automotive, and industrial applications. Ceramic particles like SiC, B4C, Al2O3, ZrB2, TiO2, Si3N4, etc., are one of many possible materials for the reinforcement particles utilized in AMMCs [1–13]. It is important to consider the intended

usage and qualities of the composite when choosing the reinforcing material. Multiple techniques, including hot pressing, powder metallurgy, and stir casting, are available for the production of AMMCs. For reinforcement, a common technique is stir casting, which entails combining molten aluminium with fibers or particles, and then pouring the mixture into a mold to harden. When compared to alternatives like powder metallurgy and hot pressing, this process has several benefits. The low production costs are a major selling point of stir casting. This process for making AMMCs is easy, cheap, and doesn't need any specialized tools or extreme temperatures. This lowers the barrier to entry for many firms, particularly those working with smaller batches. Stir casting also makes it possible to use inexpensive and easily accessible reinforcing components like metal and ceramic particles, which contributes to the cheap manufacturing cost. The reinforcing particles or fibers may be well mixed with the aluminium matrix during the stir casting process, which is an additional benefit [14–16][43]. Achieving constant mechanical qualities in the end product relies on a homogeneous distribution of reinforcement across the composite, which is achieved in this way. The ability to maintain a constant level of product quality throughout time is another advantage for manufacturers. Since stir casting is not too complicated, it is easy to increase production volumes without compromising quality. Because of this, it is perfect for use in manufacturing.

Stir casting also makes it possible to customize the composite's characteristics to a certain application by allowing the user alter the volume proportion of reinforcing particles or fibers. Factors such as the process of composite production, the size, type, and volume proportion of reinforcing particles or fibers affect the attributes of AMMCs [16]. Most of the time, AMMCs have better mechanical characteristics than pure aluminium matrices, including greater strength, modulus, as well and toughness. The properties of AMMCs, such as their high modulus, minimal thermal expansion, and great wear resistance, make them extremely adaptable and potentially useful in many applications. High strength, low weight, and resistance to wear are all things that are often needed in the aircraft, automobile, and industrial businesses. The behaviour of aluminium metal matrix composite (AMMC) under various wear circumstances may be better understood with the use of a wear study. Given the importance of wear resistance in many industries, including automotive and aerospace, this data is critical for assessing AMMC's potential use in these sectors. To further enhance AMMC's wear resistance, the wear study aids in determining the ideal matrix and reinforcing material combination. Furthermore, it may provide light on wear processes, which can lead to the creation of novel approaches to enhancing AMMC's resistance to wear [17–20]. The impact of SiC on the mechanical and microstructural characteristics was studied by Surya et al. [21] after they used a powder metallurgy process to create an Al7075/SiC composite. The primary effects of SiC particle clustering on hardness and impact strength values have been determined. A hardness value of 15 wt.% was found to be ideal. The impact of adjusting the temperatures for sintering and reinforcement on the properties of AA6061/SiC composites was studied by Surya et al. [22]. Incorporating 15% SiC particles into the composites during sintering at 406 degrees Celsius resulted in improved hardness.

Engineering has found numerous uses for PSO, including optimizing the tribological wear behaviour of metal matrix composites (MMCs). Multi-material composites (MMCs) include metal, ceramic, or polymer particles embedded in a metal matrix. Their low density, great

wear resistance, and high strength make them ideal for a number of industrial uses. Selecting the ideal mix of material qualities and manufacturing settings is a difficult task when trying to optimize the tribological wear behaviour of MMCs. When it comes to material scheduling solutions, however, the fundamental PSO algorithm does have a few limitations. In the beginning, PSO starts with a randomly generated group of particles called an "initial swarm." If the initial swarms are not spread out properly in the search region, it will not only make it harder to find the global optimal solution in three-dimensional space, but it will also have a direct effect on the stability of the algorithm [23][31][33][38][44]. However, when faced with complicated issues like material optimization, the PSO algorithm may easily get stuck in local optima as a result of random variations or constant inertial weights [24][35][40]. We provide an improved PSO (I.P.S.O) method that fixes the previous version's issues and makes the process adaptive by optimizing the initial swarm using the good point set approach. The inertial weights are then dynamically adjusted using the adaptive function to improve the algorithm's convergence.

The optimization of metal matrix composites' tribological wear behaviour using IPSO methods has many advantages, such as a global search capability, efficiency, dependability, flexibility, and the capacity to tackle optimization issues with multiple objectives [25]. For these reasons, IPSO is an appealing optimization approach for enhancing the functionality of MMCs in a wide range of engineering domains.

2. Related Works

In their study, Blaža et al. [26] used optimization approaches to examine the nanocomposite's wear rate after fabricating an A356 aluminium alloy metal supplemented with Al2O3 by means of the compo-casting process. The outcomes showed that RSM and P.S.O techniques were the most effective in obtaining the process parameter with the lowest wear rate, with an error margin of less than 10%. With a load of 100N, a speed of 1 m/s, and 0.44 wt.% Al2O3, the best results were achieved. Based on statistical analysis, they [27] optimized the wear parameters utilizing liquid metallurgical technique. The best combination of sliding distance (m), load (N), and SiC content (%) for minimizing wear loss in composites was found to be 7.5% SiC, 10 N. The SEM analysis, however, proved that the formation of deep grooves was due to the high weight percentages of hard reinforcements. Furthermore, it demonstrated enhanced matrix-reinforcement bonding. This research examined the dry sliding wear characteristics of the SiC-reinforced LM13 aluminium alloy using Design of Experiment Methodology proposed by Taguchi. Applying a weight had the greatest influence, followed by reinforcement, sliding speed, and distance, as shown by ANOVA results [28]. The tribological behaviour of the AA7075/SiC composite material was studied by Surya et al. [29] employing ANN and ANOVA methodologies. Findings show that applied force, sliding distance, and weight % SiC content are the variables most strongly influencing results. The results of the ANN study showed a very low error rate. There was an appearance of consistency between the model's estimates and the actual results. In [30], they used the stir casting technique to make a hybrid composite (Al6351 + Al2O3 + TiO2) and then adjusted the wear process parameters with the help of ANOVA and TOPSIS. During testing, the quantity of composite material that was worn away was influenced differently by load and reinforcement, according to the ANOVA findings. In contrast, TOPSIS results indicated that the sample containing (Al6351 + 10wt.% Al2O3 + 10wt.% TiO2) would exhibit the least

amount of wear. In [28], they enhanced wear process characteristics of an Al7075 + SiC + Al2O3 hybrid composite by using a statistical analysis technique. Research has shown that the wear rate and coefficient of friction are significantly affected by the weight % of reinforcing particles. In the first situation, we found that 7.5 wt.% SiC, 10N load, and 500 m distance resulted in lowest wear loss and coefficient of friction. In the second case, we found that 2.5 wt.% SiC, 30N load, and 1000 m distance produced best results. The results of the literature review indicate that there has been a lack of comparative exploration into the effects of various reinforcements on microstructure and wear behaviour up until recently. A consideration has been given to this particular aspect of the situation. Consequently, two different types of nano MMCs were prepared for this study using the stir casting process. One type had an A356 matrix with three weight percent SiC reinforced particles, while the other kind had TiO2 reinforced particles. Both an analysis of variance (ANOVA) along with the IPSO technique were used to research and assess the best configurations for the wearing process parameters.

3. Materials and Methods

In this study, SiC and TiO2 nanoparticles were used, with A356 serving as the basic alloy matrix. Characteristics of silicon carbide (SiC) nanoparticles include a low thermal expansion coefficient, excellent wear resistance, high purity, and strong thermal conductivity. But titanium dioxide (TiO2) nanoparticles have properties including being strong, resistant to wear, and having minimal toxicity. For the reinforcement components, these were chosen. In A356 you may find the following alloying elements: Zn-0.02, Mg-0.45, Cu-0.04, Fe-0.22, Si-7.1, Ti-0.1, and Al-balanced [32]. A356 is a popular aluminium alloy for high-performance uses due to its excellent corrosion resistance and high strength-to-weight ratio. By incorporating reinforcing components into the aluminium alloy, the alloy's mechanical properties, including rigidity, strength, and resistance to wear, may be further improved. In metal matrix composites (MMCs), reinforcing materials such as silicon carbide (SiC) and titanium dioxide (TiO2) are often used. To increase A356's resistance to wear, SiC is a great material to use because of its high melting point, strength, and hardness. In order to enhance the characteristics of MMCs in high-temperature applications, TiO2 is an excellent choice since it is not only hard and strong but also resistant to thermal shock and lightweight. Because of this, it is perfect for uses in the aerospace and military sectors that need top performance even when subjected to extreme environments.

3.1 Fabrication Process

Making composites from a combination of two or more components in a liquid solvent is possible using the stir-casting (Make: Swam Equip) technique. By incorporating SiC and TiO2 nanoparticles into a base alloy matrix, this approach is used to fabricate a kind of nanocomposite materials. The first thing that needs to be done is to heat the TiO2 and SiC nanoparticles through 450ºC. Before being stir-cast, the nanoparticles must be well diverse with the A356 alloy matrix. In order to achieve desirable improvements in qualities like strength and stiffness, it is crucial to thoroughly disseminate the nanoparticles completely in the base the matrix material. After melting base alloy, add nanoparticles and stir to combine. The speed at which the stirrer is set is 650 ± 25 rpm. To confirm that the nanoparticle is evenly distributed throughout base matrix material, this speed was selected. It is also

possible that the rapid speed of the stirrer supports to avoid any clump of the nanoparticles, which may have a detrimental influence on the qualities of the composite material that is ultimately produced. A cylindrical mold chamber measuring (25 mm*150 mm) is used to cast the molten material together with nano SiC and TiO2 particles after the appropriate quantity of stirring has been applied. The term for this method of molding the material into the required shape is casting. The generated composites were designated as S-0 for the basic alloy matrix, S-1 for theA356/3 wt. percent nanoTiO2 composite, and S-2 for the A356/3 wt. percent nano SiC composite.

3.2 Morphological Study

In this phrase, the steps for preparing and evaluating stir-casting composite material samples are explained. To start, we need to get the samples ready by grinding them using a belt grinder and abrasive sheets of varying grits. This process evens out the samples' surfaces and gets rid of any rough spots. Disc polishers embedded with 1.5 μm of diamond paste are then used to polish the samples. To get a surface smooth enough for microstructural analysis, this procedure is carried out. The glossy effect is achieved by the diamond paste's fine abrasive properties. In the last step, the samples that have been polished are etched using Keller's reagent, which is a combination of distilled water, hydrochloric acid, nitric acid, and hydrofluoric acid. The samples are cleaned in this way so that the grains of the substance may be seen. The atomic structure of a material may be revealed via etching, making it an essential tool for microstructure research. The next step is to analyse the materials' microstructural behaviour using ANOVA and hardness testing.

3.3 Mechanical and Wear Behaviour

The Vickers hardness tester was used to measure the hardness of the materials. To conduct the test, the composite sample were clamped down with a 100-g force for a duration of 15 seconds. The Vickers microhardness of each specimen was obtained by taking an average of three separate readings taken at different locations. The Pin-on-Disc device was used to study the wear behaviour of nanocomposites. The ASTM G99 standard was followed throughout sample processing, and the counter disc was made of EN31 steel. The weight of each of the samples was compared before and after every tribo-test to estimate the wear rate. To remove any leftover residue from surface of counter disc, it was cleaned by acetone in among each experiment. Three samples were evaluated for each condition in the wear experiment, for a grand total of 81 samples, all conducted in dry sliding conditions. We evaluated wear behaviour under different weights, sliding. distances and speeds and performed traction experiments at room temperature.

4. Experimental Design

In experimental design, the Taguchi methodology is a tool for determining how different variables affect process quality or optimization effectiveness. Here, we used the method in a controlled environment, where we could change several variables to see how they affected the result. The L27 orthogonal array, a specific design employed in the Taguchi technique, was used to create the experiment. Reduce the number of iterations needed to find the ideal values of the components under study by using this array type. In Table 1 we can see the experimental layout for the three-level controllable variables. With a lower signal-to-noise

ratio being the primary goal, the 'Smaller is Better' approach was adopted to decrease the rate of wear. The signal-to-noise ratio (S/N) may be calculated using the Equation (1) formula:

$$\frac{S}{N} = -10log\frac{1}{n}\left\{\sum y^2\right\} \quad (1)$$

Here, "y" represents the value of response, while "n" is the total test number.

Table 1 Parameters Setting

SI. No	Factors	Levell	Level2	Level3
1	Sliding Speed (m/s)	1	2	3
2	Load(N)	10	20	30
3	Sliding Distance(m)	500	1000	1500

4.1 Improvement PSO Algorithm.

An optimization technique known as Improved Particle Swarm Optimization (IPSO) finds the global optimum value of a function by simulating the behaviour of a swarm of particles as they move across a predetermined region. To solve the model, an enhanced PSO method is proposed. Firstly, the good point set optimizes the initial distribution of the particle swarm, which improves PSO search effect. Here, the adaptive dynamic functions are utilized to optimize the iterative process and the convergence effect. The second way is by optimizing the inertial weights.

4.1.1. Initialization

Good point setting is based on the following principle: set S-dimensional Euclidean space, G_s is a unit cube if $r \in G_s$, the collection of points in $G_s$can be represented in Equation(2)

$$p_n(k) = \{(\{r_1^n . k\}, \{r_2^n . k\}, \dots, \{r_s^n . k\}), 1 \le k \le n\} \quad (2)$$

The excellent point set is $p_n(k)$ if the deviation $\varphi(n)$ of $p_n(k)$ is less than or equal to $\varphi(n) = C(r,\varepsilon)n^{-1+\varepsilon}$, where $C(r,\varepsilon)$ is a constant connected to r and ε and $\varepsilon > 0$.

Results produced by employing good point sets are much better than random approaches for point set objects with n unknown disseminations, as shown in preceding theorem [34]. The good location set may better enable calculation of high-dimensional spaces since $\chi(n)$ is only connected to n for deviation, regardless of spatial dimensionality of the sample [36]. This quality of the excellent point set allows it to provide the IPSO algorithm a more suitable initial distribution approach.

Assuming an initial IPSO algorithm with n parameters, a good point set PSO approach involves selecting n points in s-dimensional space to serve as the particles' starting positions. When p is such that $(p-3)/2 \ge s$, the lowest prime number, then r is the good point, and this is shown in this research using the cyclotomic field approach, which is defined as $r = \left\{2\cos\left(\frac{2\pi\mu}{p}\right), 1 \le \mu \le s\right\}$. Each and every one of the points in Equation (2) follows a normal distribution over the interval [0, 1]. The Equation (2) becomes like Equation (3)

$$x_i(j) = \left(ub_j - lb_j\right).\left\{r_j^i . k\right\} + lb_j \quad (3)$$

In Equation (2), the upper and lower boundaries of j dimensions are represented by ub_j and lb_j, respectively. Create an initial PSO distribution with a decent set of points between 0 and 40 for $s < 3$ and $n < 100$. The distribution of data points under random circumstances is shown in Figure 1, whereas the distribution after using the circle tangent technique is shown in Figure 2.

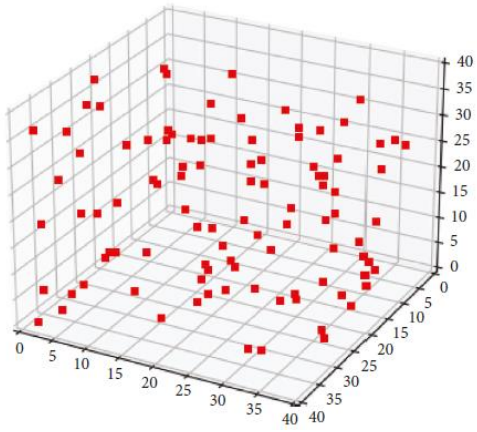

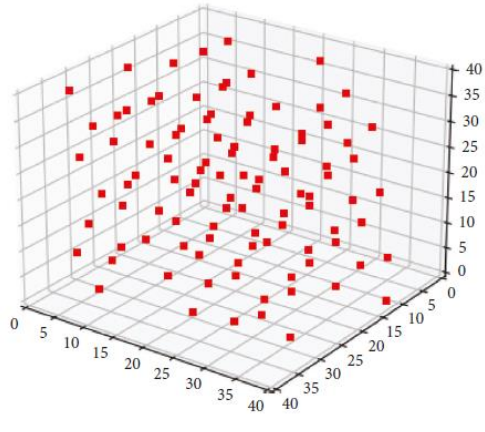

Figure 1Random Distribution Figure 2 Cyclotomic field method-based Distribution

If we compare the aforementioned application theorem with Figures 1 and 2, we can see that the random technique produces less evenly distributed particle points $\chi(n)$ for n particle objects whose distribution is uncertain. On the other hand, these particles point deviations produce more uniformly distributed particle points. Thus, the PSO algorithm's particle swarm distribution may be better allocated initially due to this excellent point set feature, leading to higher solution space coverage when developing a global particle solution. In addition, the excellent point set's allocation impact is constant for constant n, therefore it may provide the PSO algorithm a more stable initial swarm allocation scheme.

4.1.2 Inertial Weights

One of the most important things that determines the search results and the pace of convergence is the balance between global and local search skills, which are typically maintained via inertial weights [37]. Adaptive changes are made to the inertial weights of the PSO algorithm to address the issues of slower convergence with local optimality in complicated search environments. Hence, this work enhances the inertial weights in accordance with previous research [39] by dynamically adjusting the inertial weights according to the values of the goal function [37], which are stated as follows:

The maximum and minimum inertial weights are denoted by w_{max} and w_{min}, respectively, in the above equation. The objective function value for the current iteration is denoted by f, the minimum value by f_{min}, and the average value by f_{avg}.

Theoretically, it is shown that the goal function's initial weight value is set dynamically. Additionally, the global search ability is enhanced when the objective function value in the current iteration is greater than the average objective function value, and the inertial weight

value is set to its maximum. In response to swarm search feedback, the inertial weight value is lowered when the objective function value is less than the average objective function value, enhancing the local search ability.Compared to setting the inertial weights for the objective function at a fixed or random value, dynamic setting them is more beneficial for improving the algorithm's resilience and convergence when dealing with complicated issues.

4.1.3 IPSO

To address the issues with emergency material scheduling, we offer GP-APSO, an improved PSO algorithm that uses an adaptive function to set the initial weights and initializes the required particles with an even distribution of good point sets. The Pseudocode for improved PSO(IPSO) is given in in Algorithm 1.

Algorithm 1 -Improved PSO

Primary Initialization:There are N particles, s dimensions, n types of materials, z types of support points, m demand points, and m support points.

1: while:In s-dimensional space, evenly disperse n particles using the set of excellent spots as a guide.

2: A particle's location in the space may be determined using Equation (3).

3: Initiation particle velocities created at random within a certain range

4: Calculate the adaption values to find p-best and g-best when the termination condition is not satisfied:

5: For In allparticle,

6: Evaluate the fitness of each particle.

7: Determine fitness value.

8: If the fitness does not provide a workable solution,

9: Apply a severe penalty with a higher value.

10: Make the present value to the new p-best

11: For End

12: Assign a value of "g-best" to the particle that has the highest fitness rating among all of them. Revise the velocities, locations, and weights of the particles:

13: For all Particles

14: Determine particle weight

$$If\ f_{avg}\ \geq f$$

$$w = w_{max} - (w_{max} - w_{min}) \times \frac{(f - f_{min})}{f_{avg} - f_{min}}$$

$$If\ f_{avg} < f$$

$$w = w_{max}$$

15: Update the particle locations and velocities

16: End

17: End while

---

5. Experimental Results

5.1 Analysis on Hardness

A Vickers microhardness test revealed a substantial improvement in the material's microhardness. A nanoparticulate-strengthened composite's hardness is higher than that of the A356 matrix alloy. To find the hardness of the material, we focused the force on a small area as well as controlled the dispersion density such that the load wouldn't rise over the indentation zone. Figure 3 shows that compared to the bare A356 matrix alloy, microhardness of the S-1 and S-2 is increased by the value of 52.19% and 42.27 %, respectively, with the inclusion of TiO2 and SiC nanoparticles. The increased hardness of the produced composites could have several causes. To start, nanoparticles have a greater hardness than the matrix alloy; hence, the overall hardness of the matrix is increased when these reinforcements are dispersed equally throughout. Second, the hardness values of the composites are increased because the hard ceramic particles increase the dislocation density of the matrix reinforcement interfaces [41]. Finally, addition of reinforcing particles made produced composites heavier. The hardness of the composites is directly proportional to their mass, as more mass causes densification [42].

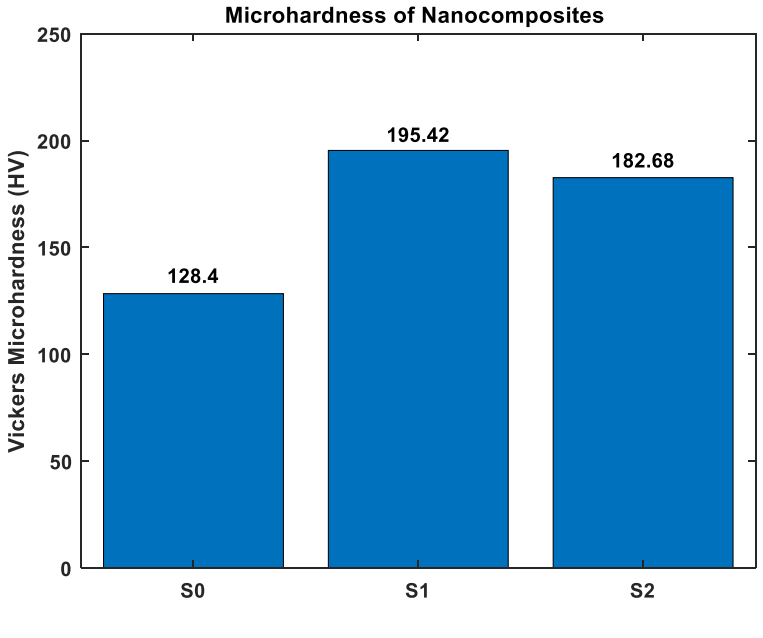

Figure 3 Microhardness of Nanocomposites

As can be seen in Figures 4 a, band c, the base alloy matrix contains equally distributed TiO2 and SiC reinforcements. Achieving this outcome is important because grain refinement is directly related to the substance being distributed evenly throughout the grain. Grain refining has been improved as a result of the incorporation of reinforcing particles into the matrix. This is due to the fact that the reinforcing particles facilitate the formation of smaller grains

by acting as a barrier, which in turn prevents the growth of too large grains. A very robust reinforcement-matrix association exists. The development of big grains and grain size are both successfully halted by the spread of nanoparticles. The pinning effect is greater for smaller particles than larger ones.

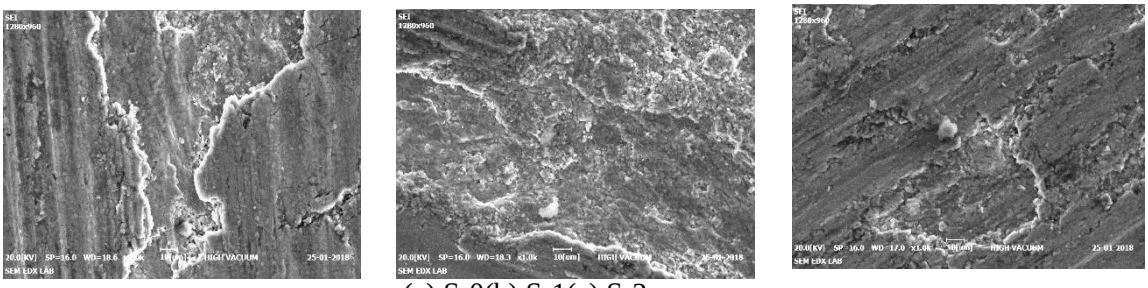

(a) S-0(b) S-1(c) S-2

Figure 4 SEM micrographs ofnanocomposites

5.2 ANOVA Analysis

To ensure that all data collection was done in a controlled way, the experiment's testing parameters and their levels were calculated using the Taguchi standard (L27) orthogonal array. The effects of sliding speed, load and distance on the wear rate of S0, S1, and S2 nanocomposites have been examined using analysis of variance. For the purpose of the wear rate analysis, "smaller is better" and "identical response" are selected as criteria. Tables 2,3 and 4demonstrates the results of the analysis of variance. A 95% level of confidence was established for the analysis's results. The examination of the variance for the base matrix alloy A356 is shown in Table 2. We find that sliding distance is the most important factor affecting wear rate (63.11%), followed by Speed 16.41% and Load 14.17%. Table 3 shows that in an analysis of variance for A356+ 3wt.% TiO2 composite, the component with the most effect on the wear rate is the applied load (P = 41.71 %), while sliding speed has a 34.45% impact and sliding distanceis16 % impact. Results for A356 + 3wt.% SiC are shown in Table 4 for the analysis of variance. Research shows that the sliding speed (37.81%) and applied load (37.4%) are the two most important factors influencing the wear rate. The wear rate is affected by the sliding distance to the tune of 17.84%. The relationships between the three process factors had a little influence on the overall outcome. It has been noted that all three composites have a residual error rate below 2%. S-0, S-1, and S-2 composites all achieved R2 values of 99.18%, 99.68%, and 98.41%, respectively. There is a significant link between both dependent and independent variables, as shown by the high R-squared value.

Table 2 Base A356 Variance Analysis

Source	DF	Seq SS	Adj SS	Adj MS	F	P	% Impact
Load(N)	2	7.1547	7.1547	3.9852	77.24	0.000	14.17
Speed(m/s)	2	9.4781	9.4781	4.1754	89.21	0.000	16.41
Distance(m)	2	34.1874	34.1874	16.4257	331.74	0.000	**63.11**
Load(N)*Speed(m/s)	4	0.1687	0.1687	0.0387	0.72	0.533	0.298
Load(N)*Distance(m)	4	0.0641	0.0641	0.0174	0.31	0.731	0.127
Speed(m/s) *Distance(m)	4	1.1487	1.1487	0.247	5.12	0.019	1.985
Residual Error	8	0.4103	0.4103	0.0412			0.72
Total	26	52.612					
R-Sq 99.18% R-Sq(adj)	96.87%						

Table 3 Base A356 + 3w.t %TiO2 -Variance Analysis

Source	DF	Seq SS	Adj SS	Adj MS	F	P	% Impact
Load(N)	2	16.9045	16.9045	8.86014	566.57	0	**41.71**
Speed(m/s)	2	15.0507	15.0507	6.96165	475.29	0	34.45
Distance(m)	2	6.3501	6.3501	2.507	226.06	0	16
Load(N)*Speed(m/s)	4	0.6217	0.6217	0.15193	9.79	0.008	1.46
Load(N)*Distance(m)	4	1.0177	1.0177	0.25576	16.18	0.001	2.423
Speed(m/s) *Distance(m)	4	0.1401	0.1401	0.00512	2	0.136	0.211
Residual Error	8	0.1163	0.1163	0.00443	0	0	0.25
Total	26	40.2012	0	0	0	0	0
R-Sq 99.68% R-Sq(adj)	98.95%						

Table 4 Base A356 + 3w.t %SiC -Variance Analysis

Source	DF	Seq SS	Adj SS	Adj MS	F	P	% Impact
Load(N)	2	15.0331	15.0331	7.92446	90.53	0	37.4
Speed(m/s)	2	16.2875	16.2875	7.58004	91.45	0	**37.81**
Distance(m)	2	7.0987	7.0987	2.88128	43.64	0	17.84
Load(N)*Speed(m/s)	4	0.2774	0.2774	0.06584	0.69	0.545	0.652
Load(N)*Distance(m)	4	0.5232	0.5232	0.13216	1.47	0.179	1.253
Speed(m/s) *Distance(m)	4	0.1478	0.1478	0.00321	0.06	0.769	0.238
Residual Error	8	0.6939	0.6939	0.07662	0	0	1.62
Total	26	40.0616	0	0	0	0	0
R-Sq 98.41% R-Sq(adj)	99.01%						

In order to monitor how well the process settings were working, the collected data was converted to a signal-to-noise ratio. Finding the signal-to-noise ratio required studying how the process control parameters affected the wear rate and frictional coefficient. The ratio of SNR for the wear rate at different levels of analysis parameters is used to rank the parameters, and the results are shown in Tables 5, 6, and 7. In terms of S-0, the order of

importance is as follows: composite sliding distance at 1, speed at 2, and load at 3. In the same way, for S-1, speed and distance come in order of preference, with the composite applied load ranking first. Composite sliding speed is the most important factor for S-2, followed by weight and distance. One way to see the connection between the two sets of variables in an Analysis of Variance (ANOVA) is using a main effects plot for average values, which is also called a main effects graph. For each level of the independent variables, it displays the dependent variable's mean. With the x-axis representing the independent variable and the y-axis representing the dependent variable, the graph takes the form of a line.

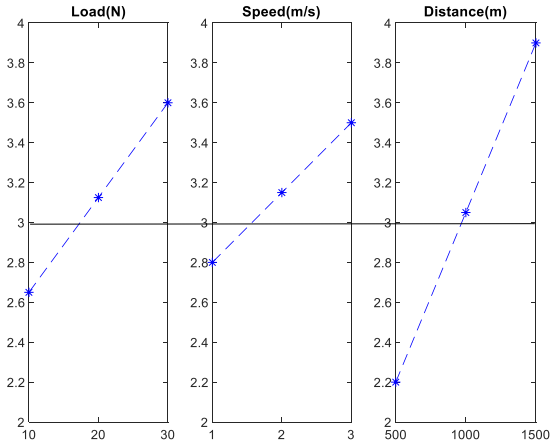

Figure 5 Wear Rate Analysis for S0

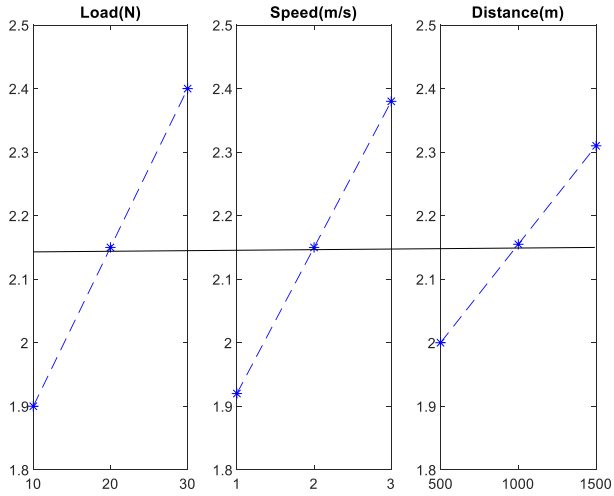

Figure 6 Wear Rate Analysis for S1

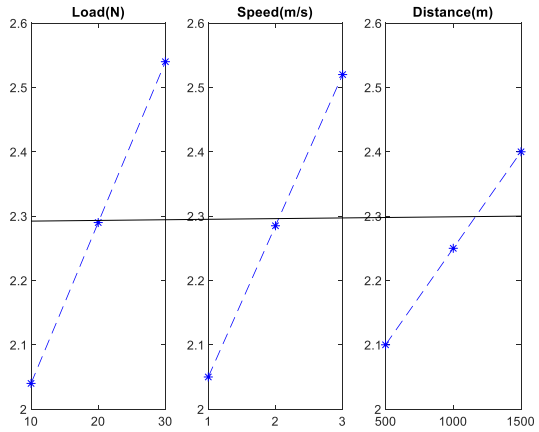

Figure 7 Wear Rate Analysis for S2

Figures 5, Figure 6 and Figure 7 show the average wear rate for S0, S1, and S2 composites, respectively, as shown in the main effects plots. A parameter's significance is low if its line is almost parallel to the level. A parameter's significance is highest when its line is steepest with respect to the horizontal. In Figure 5, we can see how the independent factors affected the wear rate. Among all the component's, sliding distance was determined to have the most significant slope. Therefore, the most important component influencing the wear rate is the sliding distance. The applied load and sliding speed exhibit the steepest slopes, leading to the most influencing variables (Figures 6 and Figure 7), which is consistent with the pattern.

Table 5Analysis outcomes for A356

Level	Load(N)	Speed(m/s)	Distance(m)
1	-9.154	-9.005	-8.541
2	-9.874	0.974	-9.485
3	-10.578	-10.542	-11.21
Delta	1.324	1.451	2.514
Rank	III	II	I

Table 6 Analysis outcomes for A356 +3wt.%TiO2

Level	Load(N)	Speed(m/s)	Distance(m)
1	-5.486	-5.543	-5.882
2	-6.752	-4.67	-6.478
3	-7.572	-7.456	-7.081
Delta	1.987	1.828	1.043
Rank	I	II	III

Table 7 Analysis outcomes for A356 +3wt.%SiC

Level	Load(N)	Speed(m/s)	Distance(m)
1	6.136	-5.886	-6.256
2	-7.14	-5.116	-6.87
3	-7.926	-7.869	-7.517
Delta	1.88	1.897	1.106
Rank	II	I	III

5.3 Confirmation test

From the optimum values of (Tables 5,6, and 7), we executed confirmation tests. Table 8 illustrates results of these tests along with a comparison to ideal values. The error in calculating the wear rate of any material is less than 5%, according to results. Consequently, the results support the reasonable level of extrapolation.

Table 8 Confirmation Test

Output Response	Experimental Value	Predicted Value	Error%
Wear Rate (1*10-3mm3/m)			
S-0	2.25	2.207	4.3
S-1	1.6842	1.6778	0.64
S-2	1.7467	1.7142	3.25

5.4 IPSO Analysis

Key considerations in developing this formulation include the following: a minimum of 0.4, a maximum of 0.9, a lower limit of [10, 1, 500], and an upper bound of [30, 3, 1500]. In addition, the number of swarm particle sizes was set at 50. Furthermore, Table 9 explains the optimum outcomes achieved by using the IPSO approach, as well as the details of the experimental data values used for comparison. Results showed very high levels of consistency overall, with expected and observed values matching with each other. Overall, the variances ranged from 4 to 7%, and there were just a few insignificant variations. The strategy has a 93% success rate; therefore, it must be resilient. It seems like this procedure produces rather reliable findings.

Table 9 Analysis of IPSO

Specimens	Predicted Values	Experimental Values	%Error
S0	2.2987	2.2547	4.4
S1	1.6747	1.6187	5.6
S2	1.7814	1.714	6.74

6. Conclusion and Future Enhancement

The A356 alloy matrix was successfully enhanced with 3 weight percentage of TiO2 and 3 weight % SiC nanoparticles using the stir-casting technique. According to the results of the analysis of variance (ANOVA), the sliding distance has the greatest impact on the wear rate of the base matrix alloy (63.11 %), followed by the speed and the load. Wear rate is most affected by applied load (41.71%), then by speed and distance, in the case of a 3wt.% TiO2 reinforced nanocomposite. When it comes to 3wt.% SiC nanocomposite, sliding speed is the most important factor affecting wear rate at 37.81%, followed by load and distance. To find

the maximum feasible wear rate, the IPSO optimization method was used. An error rate of less than 8.5% was found in the confirmation test, keeping it below the range that is appropriate.

References

[1] HU K, YUAN D, LÜ S lin, WU S sen (2018) Effects of nano- SiCp content on microstructure and mechanical properties of SiCp/A356 composites assisted with ultrasonic treatment. Trans Nonferrous Met Soc China (English Ed 28:2173–2180. https:// doi. org/ 10. 1016/ S1003- 6326(18) 64862-9

[2] Sahoo AK, Pradhan S (2013) Modeling and optimization of Al/SiCp MMC machining using Taguchi approach. Meas J Int Meas Confed 46:3064–3072. https:// doi. org/ 10. 1016/j. measurement. 2013. 06. 001

[3] Azad MSPA (2018) Investigations on Coefficient of Friction and Surface Roughness of AA6061 + B 4 C Composites Produced by Stir Casting Process. J Mater Sci Surf Eng 6:779–782

[4] Ramadoss N, Pazhanivel K, Ganeshkumar A, Arivanandhan M (2022) Microstructural, mechanical and corrosion behaviour of B4C/BN-reinforced Al7075 matrix hybrid composites. Int J Met. https:// doi. org/ 10. 1007/ s40962- 022- 00791-z

[5] Ekka KK, Chauhan SR, Varun (2015) Study on the sliding wear behaviour of hybrid aluminium matrix composites using Taguchi design and neural network. Proc Inst Mech Eng Part L J Mater Des Appl 230:537–549. https:// doi. org/ 10. 1177/ 14644 20715 581393

[6] Chen M, Liu Z (2020) Ultrasound assisted casting method for fabricating B4Cp/Al composites with the addition of K2ZrF6. Mater Lett 280:128545. https:// doi. org/ 10. 1016/j. matlet. 2020. 128545

[7] Dv N, Bk B, Gk M (2020) Microstructure, mechanical properties and fracture mechanisms of ZrB2 ceramic reinforced A7075 composites fabricated by stir casting. Mater Today Commun 25:101289. https:// doi. org/ 10. 1016/j. mtcomm. 2020. 101289

[8] Ramkumar KR, Natarajan S (2019) Effects of TiO2 nanoparticles on the microstructural evolution and mechanical properties on accumulative roll bonded Al nanocomposites. J Alloys Compd 793:526–532. https:// doi. org/ 10. 1016/j. jallcom. 2019. 04. 218

[9] Bharat N, Bose PSC (2022) Influence of nano-TiO2 particles on the microstructure, mechanical and wear behaviour of AA7178 alloy matrix fabricated by stir casting technique. Proc Inst Mech- Eng Part L J Mater Des Appl 14644207221123520. https:// doi. org/ 10. 1177/ 14644 20722 11235 20

[10] Mohanavel V, Ravichandran M (2021) Optimization of Parameters to Improve the Properties of AA7178/Si3N4 Composites Employing Taguchi Approach. Silicon 1381–1394. https:// doi. org/ 10. 1007/ s12633- 020- 00917-0

[11] Kumar A, Rana RS, Purohit R (2022) Microstructure evolution, mechanical properties, and fractography of AA7068/ Si3N4nanocomposite fabricated thorough ultrasonic-assisted stir casting advanced with bottom pouring technique. Mater Res Express 9 https:// doi. org/ 10. 1088/ 2053- 1591/ ac4b78

[12] Suresh S, Natarajan E, Franz G, Rajesh S (2022) Differentiation in the SiC Filler Size Effect in the Mechanical and Tribological Properties of Friction-Spot-Welded AA5083-H116 Alloy. Fibers 10

[13] Suresh S, Elango N, Venkatesan K et al (2020) Sustainable friction stir spot welding of 6061–T6 aluminium alloy using improved non-dominated sorting teaching learning algorithm. J Mater Res Technol 9:11650–11674. https:// doi. org/ 10. 1016/j. jmrt. 2020. 08. 043

[14] Samal P, Kumar R, Pandu M (2020) Dry sliding wear behavior of Al 6082 metal matrix composites reinforced with red mud particles. SN Appl Sci 2:1–11. https:// doi. org/ 10.

1007/ s42452- 020- 2136-2

[15] Aynalem GF (2020) Processing Methods and Mechanical Properties of Aluminium Matrix Composites. Adv Mater Sci Eng 2020 https:// doi. org/ 10. 1155/ 2020/ 37657 91

[16] Bharat N, Bose PSC (2021) An overview of production technologies and its application of metal matrix composites. Adv Mater Process Technol. https:// doi. org/ 10. 1080/ 23740 68X. 2021. 18787 07

[17] Kumar J, Singh D, Kalsi NS et al (2021) Investigation on the mechanical, tribological, morphological and machinability behavior of stir-casted Al/SiC/Mo reinforced MMCs. J Mater Res Technol 12:930–946. https:// doi. org/ 10. 1016/j. jmrt. 2021. 03. 034

[18] Meti VKV, Konaraddi R, Siddhalingeshwar IG (2018) Mechanical and Tribological Properties of AA7075 Based MMC Processed through Ultrasound Assisted Casting Technique. Mater Today Proc 5:25677–25687. https:// doi. org/ 10. 1016/j. matpr. 2018. 11. 009

[19] Udaya Prakash J, JebaroseJuliyana S, Saleem M, Moorthy TV (2021) Optimisation of dry sliding wear parameters of aluminium matrix composites (356/B4C) using Taguchi technique. Int J Ambient Energy 42:140–142. https:// doi. org/ 10. 1080/ 01430 750. 2018. 15255 90

[20] Bharat N, Bose PSC (2021) An overview on the effect of reinforcement and wear behaviour of metal matrix composites. Mater Today Proc. https:// doi. org/ 10. 1016/j. matpr. 2020. 12. 084

[21] Surya MS, Prasanthi G (2022) Effect of Silicon Carbide Weight Percentage and Number of Layers on Microstructural and Mechanical Properties of Al7075/SiC Functionally Graded Material. SILICON 14:1339–1348. https:// doi. org/ 10. 1007/ s12633- 020- 00865-9

[22] Surya MS, Kumar VN, Sridhar A (2022) To Study the Effect of Varying Sintering Temperature and Reinforcement on Physical and Mechanical Characteristics of AA6061/SiC Composites. SILICON. https:// doi. org/ 10. 1007/ s12633- 022- 02233-1

[23] [11] A. Ashraf, A. Ali Almazroi, W. Haider Bangyal, and MAlqarni, "Particle swarm optimization with new initializingtechnique to solve global optimization problems," Intelligent Automation & Soft Computing, vol. 31.1, pp. 191–206, 2022.

[24] [12] S. K. Sahana and S. K. Sahana, "Ba-PSO: a Balanced PSO to solve multi-objective grid scheduling problem," Applied Intelligence, vol. 52.4, pp. 4015–4027, 2022.

[25] 26. Alajmi MS, Almeshal AM (2020) Prediction and Optimization of Surface Roughness in a Turning Process Using the ANFISQPSO Method. Materials (Basel). 13

[26] 27. Stojanović B, Gajević S, Kostić N et al (2022) Optimization of parameters that affect wear of A356/Al2O3 nanocomposites using RSM, ANN, GA and PSO methods. Ind LubrTribol 74:350–359. https:// doi. org/ 10. 1108/ ILT- 07- 2021- 0262

[27] 28. Ravikumar M, Reddappa HN, Suresh R et al (2022) Optimization of wear behaviour of Al7075/SiC/Al2O3 MMCs Using statistical method. Adv Mater Process Technol 8:4018–4035. https:// doi. org/ 10. 1080/ 23740 68X. 2022. 20365 83

[28] 29. Khan MM, Dey A, Hajam MI (2022) Experimental Investigation and Optimization of Dry Sliding Wear Test Parameters of Aluminum Based Composites. SILICON 14:4009–4026. https:// doi. org/ 10. 1007/ s12633- 021- 01158-5

[29] 30. Surya MS, Prasanthi G, Kumar AK et al (2021) Optimization of Tribological Properties of Powder Metallurgy-Processed Aluminum7075/SiC Composites Using ANOVA and Artificial Neural Networks. J Bio- Tribo-Corrosion 7:161. https:// doi. org/ 10. 1007/ s40735-021- 00600-w

[30] 31. Ahamad N, Mohammad A, Sadasivuni KK, Gupta P (2020) Wear, optimization and surface analysis of Al-Al2O3-TiO2 hybrid metal matrix composites. Proc Inst Mech Eng Part J J Eng Tribol 235:93–102. https:// doi. org/ 10. 1177/ 13506 50120 970432

[31] Prasad Babu, P., &Vasumathi, A. (2023). Role of Artificial Intelligence in Project Efficiency

Mediating with Perceived Organizational Support in the Indian IT Sector. Indian Journal of Information Sources and Services, 13(2), 39–45.

[32] Paulraj, D., P. Jeyakumar, G. Rajamurugan and Prabu Krishnasamy. "Influence of nano TiO2/Micro (SiC/B4C) Reinforcement on the Mechanical, Wear and Corrosion Behaviour of A356 Metal Matrix Composite." Archives of Metallurgy and Materials (2023): n. pag.

[33] Bekri, M. E., Diouri, O., &Chiadmi, D. (2023). Dynamic Inertia Weight Particle Swarm Optimization for Anomaly Detection: A Case of Precision Irrigation. Journal of Internet Services and Information Security, 13, 157-176.

[34] Y. Li, Z. Ni, F. Jin, J. Li, and F. Li, "Research on clustering method of improved glowworm algorithm based on goodpoint set," Mathematical Problems in Engineering, vol. 2018, pp. 1–8, 2018.

[35] Nikitina, V., Raúl, A.S., Miguel, A.T.R., Walter, A.C., Anibal, M.B., Maria, D.R.H., & Jacqueline, C.P. (2023). Enhancing Security in Mobile Ad Hoc Networks: Enhanced Particle Swarm Optimization-driven Intrusion Detection and Secure Routing Algorithm. Journal of Wireless Mobile Networks, Ubiquitous Computing, and Dependable Applications, 14(3), 77-88.

[36] Y. Chen, X. Liang, and Y. Huang, "Improved quantum particle swarm optimization based on good-point set," ZhongnanDaxueXuebao (Ziran Kexue Ban)/Journal of Central South University(Science and Technology), vol. 44, no. 4,pp. 1409–1414, 2013.

[37] [29] S. Khan, M. Kamran, O. U. Rehman, L. Liu, and S. Yang, "A modified PSO algorithm with dynamic parameters for solving complex engineering design problem," International Journal of Computer Mathematics, vol. 95, no. 11, pp. 2308–2329, 2018.

[38] Rasanjani, C., Madugalla, A. K., & Perera, M. (2023). Fundamental Digital Module Realization Using RTL Design for Quantum Mechanics. Journal of VLSI Circuits and Systems, 5(2), 1-7.

[39] [30] W. Yi, Y. Min, and Z. Jiang, "Fuzzy particle swarm optimization clustering and its application to image clustering," in Proceedings of the Pacific Rim Conference on Advances in Multimedia Information Processing Springer-Verlag, Springer, Hangzhou, China, November 2006.

[40] Rasanjani, C., Madugalla, A. K., & Perera, M. (2023). Fundamental Digital Module Realization Using RTL Design for Quantum Mechanics. Journal of VLSI Circuits and Systems, 5(2), 1-7.

[41] 38. Madhukar P, Selvaraj N, Rao CSP, VKG B (2019) Tribological behavior of ultrasonic assisted double stir casted novel nano-composite material (AA7150-hBN) using Taguchi technique. Compos Part B 175:107136. https:// doi. org/ 10. 1016/j.compo sitesb. 2019. 107136

[42] 39 Madhukar P, Selvaraj N, Rao CSP, Veeresh Kumar GB (2020) Enhanced performance of AA7150-SiC nanocomposites synthesized by novel fabrication process. Ceram Int 4

[43] Pavel, K., Borislav, S., Dušan, J., &Ildico, M. (2022). On the Abrasive Wear High Strength Coating Layers on Machine Parts Testing. Arhiv za tehničkenauke, 2(27), 25-31.

[44] Sinha, P. (2013). Particle swarm optimization for solving economic load dispatch problem. International Journal of Communication and Computer Technologies (IJCCTS), 1(2), 100-105.